Journal of the European Ceramic Society **18** (1998) 287–297

PII: S0955-2219(97)00109-X
0955-2219/98/$19.00 + 0.00

Ultrafine Titania by Flame Spray Pyrolysis of a Titanatrane Complex

Clint R. Bickmore, Kurt F. Waldner, Rita Baranwal, Tom Hinklin, David R. Treadwell and Richard M. Laine*

Departments of Materials Science and Engineering, Chemistry, and the Macromolecular Science and Engineering Center, University of Michigan, Ann Arbor, MI 48109-2136, USA

(Received 26 March 1997; accepted 23 May 1997)

Abstract

Ultrafine titania particles can be produced by flame spray pyrolysis of a chelated metal alkoxide. The precursor can be made by reacting a titanium hydrosol with triethanolamine in ethylene glycol. The chelate, dissolved in ethanol, is misted as an aerosol into an oxidizing flame where it undergoes combustion. The combustion process generates particles, probably by a gas phase condensation process, that are discrete single crystals that exhibit some faceting. The powder is a mixture of anatase and rutile (<10%), with a $45 \pm 5\,m^2\,g^{-1}$ BET surface area. The calculated equivalent spherical diameter (34+4 nm) is consistent with typical particle sizes found in TEM micrographs. The particles are briefly compared with commercial ultrafine particles produced by flame hydrolysis of $TiCl_4$ and by Ti vapor condensation. © *1998 Elsevier Science Limited.*

Introduction

Ultrafine ceramic particles (UFPs <150 nm) have more near surface atoms than respective coarser particles (e.g. $>1\,\mu$m) giving rise to higher free energies that permit densification of bulk powders or thin films at much lower temperatures than possible with coarser powders.[1,2] The opportunity to process ceramic shapes at lower temperatures can result in lower energy and capital equipment costs, and permit processing of materials that will degrade at higher temperatures, e.g. electronic materials. The utility of UFPs in processing ceramic materials is currently constrained by the high costs of the powders that are available and the limited types of powders available (typically single metal oxides).

*To whom correspondence should be addressed.

We recently described a simple, low-cost method of producing spinel UFPs by flame spray pyrolysis (FSP) of a chelated magnesium aluminate, double-alkoxide precursor.[3] The precursor is made by direct reaction of MgO and $Al(OH)_3$ with a chelating ligand. The flame spray pyrolysis apparatus used is analogous to a fuel oil burner[4,5] adapted with a powder collector (see below). Combustion occurs at atmospheric pressure, thus minimizing equipment needs compared to powder processing by physical or chemical vapor techniques.[6,7] To demonstrate the general utility of this approach, we report here on flame spray pyrolysis processing of titania UFP and briefly compare the characteristics with commercially available nanosized or ultrafine powders.

Flame combustion takes advantage of ligand heats of combustion to convert the precursor to its corresponding metal oxide. Previous studies on flame combustion have used a wide variety of precursors including metal salts,[8,9] metallo-organics,[3,10] and metal alkyls.[11] Our approach, FSP, uses a chelated metal alkoxide made by reacting triethanolamine [TEA, $N(CH_2CH_2\,OH)_3$] with titania in ethylene glycol.

$$TiO_2 + N(CH_2CH_2OH)_3 + \text{ethylene glycol} \xrightarrow{200^\circ C/\,-\,H_2O}$$

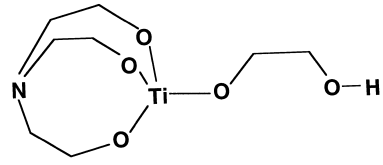

(1)

Titanatrane glycolate, the product of reaction (1), can also be synthesized via exchange reactions with common titanium alkoxides, e.g. $Ti(OiPr)_4$.[12] One

advantage of these chelated metal-alkoxides is their hydrolytic stability, which minimizes special handling requirements.[13]

FSP is very similar to fuel oil combustion[4,5,14] in that both processes combust low vapor pressure fuels by injecting a fuel aerosol into a combustion zone. Aerosol combustion begins with evaporation of the components of the fuel in the individual droplets. The components in fuel oils are various molecular weight organics. In the precursor solution, the fuel components are the alcohol solvent and the precursor ligands. Oxygen serves as both the atomizing gas in a two fluid aerosol generator and as a coreactant. Combustion provides heat to vaporize the incoming aerosol and to oxidatively decompose ligands. Once the organics are oxidized, an inorganic vapor results, which generates particles.

Vapor phase particle growth can occur via three processes: nucleation, vapor deposition, and cluster-collision.[15–18] In vapor combustion processes, oxidation of the ligands/adducts generates metal-oxide clusters that condense to form nuclei which in turn grow by consuming the vapor phase. The physical state (size and phase) of the metal-oxide species is not static, nor is it readily identifiable. As a working definition, the term 'cluster' refers to the initially generated species which form either as a vapor, liquid or solid. We further assume that these clusters are not stable in the reaction environment and will coalesce to form nuclei and it is these nuclei that form stable particles. Once formed, nuclei collisions can lead to either coalescence or aggregation, where the nuclei 'temperature,' and number density dictates the mechanism. In the combustion zone, much of the energy is transferred by radiation, producing a large temperature gradient from the combustion zone to the powder collector. Cooling changes the effect of collision from coalescence to aggregation. Aggregates contain discrete particles with neck formation at the contact zones. Collisions after further cooling form agglomerates, which are noted by the absence of necks.

Vapor phase particle formation appears to be the mechanism operative in FSP. For example, FSP of the spinel precursor produces spherical, single crystal particles with a typical particle size of 35 nm.[3] Particle formation appears to be independent of aerosol droplet size provided that heat transfer is rapid enough to combust the entire droplet within the combustion zone: The heat transfer limited case produces spurious particles similar to spray pyrolysis.[18,19] A steep thermal gradient ($>1000^{\circ}C\,m^{-1}$) in the combustion zone minimizes aggregate formation, allowing production of discrete UFP spinel at rates greater than $100\,g\,h^{-1}$.

The UFP titania produced here is potentially of value for a wide variety of applications including conventional solid-state sintering, tape casting, and as a transparent filler in polymer composites. Thus, we also briefly compare its properties with those of UFP titania produced via other methods. A second objective of this work is to produce UFP titania that can be used to produce UFP TiN by ammonolysis, which will be the subject of a later paper.

Experimental Procedures

Reagents

Titanatrane precursor can be synthesized from an aqueous hydrosol derived from $TiCl_4$, (Fluka Chemika, Rononkoma, NY). Ammonium carbonate, reagent grade, (Mallinckrodt, Paris, KY) was used to precipitate the sol. Triethanolamine (TEA, $N(CH_2CH_2OH)_3$, Dow Chemical Co., Midland, MI) was used as received (98%). Analytical grade ethylene glycol (EG, $HOCH_2CH_2OH$) and 2-butyl alcohol (Mallinckrodt, Paris, KY) were used as received. EG recovered from the reaction was redistilled to remove H_2O and recycled into the reactions. Ethyl alcohol (95%, McCormick, Weston, MO) was used as received. Commercial UFP titania (Degussa P25 and Nanophase) were obtained from several independent sources.

Titania hydrosol synthesis

A colloidal titania hydrosol was synthesized by reacting $TiCl_4$ (100 ml) with deionized water (2500 ml). In an exhaust hood, three volumes from a partially filled 50 ml syringe were added dropwise into a beaker of vigorously stirring, chilled water. *Note: hydrolysis of $TiCl_4$ is exothermic, so addition should be done cautiously*. The hue of the resulting solution ranges from colorless to colloidal blue based on the solution temperature.[20] The solution can be precipitated to form an amorphous hydrosol by raising the pH with ammonium carbonate. The hydrosol was recovered from suspension by filtering with a vacuum assisted Buchner funnel. The filter cake was then re-suspended in deionized water and stirred for 30 min. The filtration process was done 3× to minimize the chlorine content to avoid subsequent formation of triethanolamine hydrochloride [$(HOCH_2CH_2)_3N{\cdot}HCl$]. The hydrosol was transferred to the schlenkware described below, along with $\approx$500 ml of EG. The mixture was heated, under N_2, to distill off water, resulting in a titania hydrosol in EG. A TGA of the hydrosol was done to determine the equivalent TiO_2 in suspension; the ceramic yield was 3·3 wt%. The hydrosol (45·9 g, 575 mmol as TiO_2) was reacted

with 4:3 equivalents TEA:Ti (114·3 g, 766 mmol TEA) as described below.

Titanatrane glycolate, $N(CH_2CH_2O)_3TiOCH_2CH_2$-OH, synthesis

Typical reaction conditions are as follows and are discussed in detail elsewhere.[21,22] The hydrosol from above was reacted, under N_2, in a 1-liter, three-necked schlenk flask, equipped with a mechanical stirrer, and a still head. The mixture was heated to 200°C, the boiling point of EG. Over 8 h, ≈1 litre of EG and byproduct H_2O were distilled off (with periodic replenishment of EG). Concurrent with distillation, the solution became clear, indicating complete reaction, and formation of the titanatrane glycolate complex. Once the solution cleared, distillation was continued to concentrate the solution until the still head temperature reached 205–210°C, indicating most of the EG had distilled off. On cooling, an equal volume of ethanol (≈200 ml) was added to to reduce viscosity.

The precursor concentration was finally adjusted to have a drain time of 40–42 s in a capillary volumetric at 23·7°C. Drain times for deionized water and EG in the capillary were 19 and 100 s, respectively. The precursor was diluted to obtain a 5–10 wt% ceramic yield. Table 1 lists selected properties of solvents used in flame pyrolysis,[23] to adjust combustion characteristics. For example, butanol is added to increase the heat of combustion. A typical 2500 ml precursor solution contained 650 ml precursor (150 g TiO_2 yield), 400 ml butanol, 1450 ml ethanol, giving a 0·90 g cc^{-1} density and 6·7 wt% yield. At solution feed rates of 25 ml min^{-1}, the combustion of the solvent alone generates more than 7 kW of heat.

Flame spray pyrolysis

The flame spray pyrolysis (FSP) apparatus consists of an aerosol generator, a combustion chamber, and a powder collector. The generator was a twin, two fluid Bernoulli mister that used O_2 as the atomizing gas. Precursor was fed to the mister from a 1 litre reservoir maintained under 2–20 psi N_2. The aerosol was fed into the fused quartz (80 mm ID×200 mm) combustion chamber through a port in the entry face adjacent to a port holding a gas/oxygen pilot torch used to initiate and sustain ignition. The combustion chamber was connected to a parallel set of electrostatic precipitators (ESPs, 3 inch×0·125 inch Al) operated between 5 and 10 kV. Lastly, the flue gases were ducted through a countercurrent, water scrub tower ≈10 cm×150 cm.

Flame spray pyrolysis was initiated by injecting an ethanol aerosol into the combustion chamber. The feed was then changed to the precursor solution. The flame became luminous due to incandescence of the particles, and shortly thereafter, the combustion chamber became coated with powder. The temperature was monitored at a thermocouple (TC), located near the ESPs (see Fig. 1).

The titanatrane complex was flame spray pyrolyzed on two occasions: the first consisted of several intermittent runs spanning 4 h; and the second consisted of two runs 2 h each. Each occasion resulted in more than 100 g titania. Precursor flow rates were varied between 15 and 25 ml min^{-1} for the first run and 8–15 ml min^{-1} for the second. The slightly lower flow rate of the second run allowed exchange of the ESPs with continuous operation, at the expense of lower production rates (25 g $h^{-1}TiO_2$).

Characterization

Thermal analysis. Thermogravimetric analysis (TGA) and differential thermal analysis (DTA) were done on a TA Instruments Thermal Analyst 2200 with HiRes TGA 2950 (New Castle, DE). The TGA was heated at constant ramp rates (10°C min^{-1}). The TGA balance flow meter was set at 40 ml min^{-1} N_2, while the purge flow meter was adjusted to 60 ml min^{-1} of either N_2 or dry air.

DRIFTS. Diffuse reflectance infrared Fourier transform (DRIFT) spectra[24–27] were obtained on a Mattson Galaxy Series 3020 (Madison, WI) bench continuously purged with N_2, adapted with a Harrick Scientific Corp. 'Praying Mantis' Diffuse Reflectance Accessory (DRA-2CO). The non-absorbing medium used was potassium bromide (KBr, ICL, Garfield, NJ) powdered from single crystal with an alumina mortar and pestle. Powder specimens were prepared as follows:

Table 1. Properties of selected solvents

	Boiling point (°C)	*Density (g cc^{-3})*	*Viscosity[a] (mPa·s)*	*ΔH^b (kJ mol^{-1})*	*ΔH^b (kJ g^{-1})*	*ΔH^b (kJ cm^{-3})*
Methanol	65	0·7914	0·544	726·1	22·66	17·93
Ethanol	78·5	0·7893	1·074	1366·8	29·67	23·42
Isopropanol	82·4	0·7855	2·038	2005·8	33·38	26·22
2-Butanol	99·5	0·807	3·096	2660·6	35·90	28·97
Ethylene glycol	198	1·110	16·1	1189·2	19·16	21·27

[a]Viscosities of the liquid at 25°C.
[b]Enthalpies of combustion are from the liquid at 25°C.

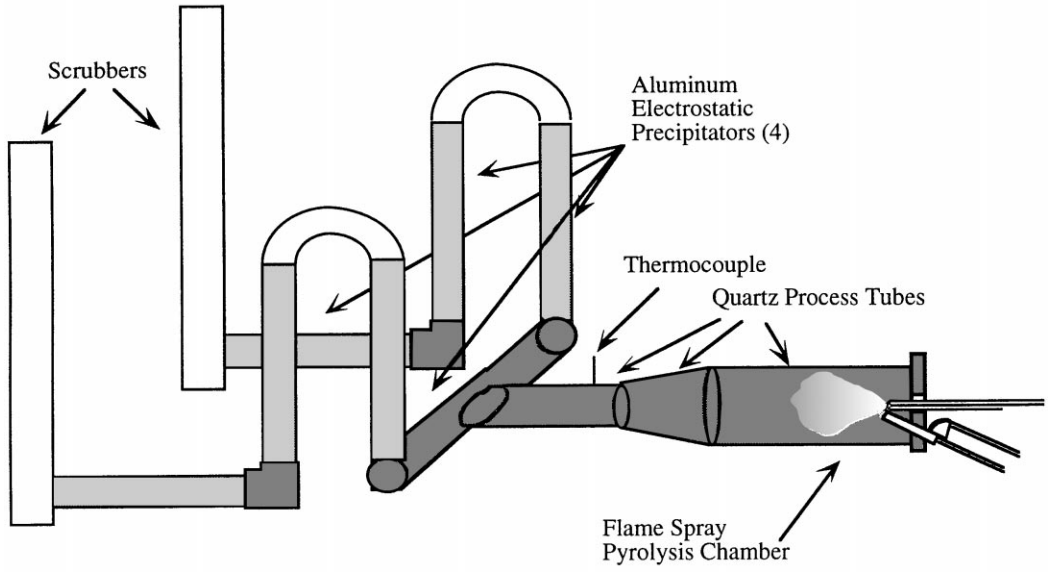

Fig. 1. Flame spray pyrolysis apparatus.

1. 0·5 wt% analyte was mixed with the KBr (e.g. 2 mg analyte to 400 mg KBr);
2. the mixture was ground rigorously with an alumina mortar and pestle; and
3. the dilute samples were subsequently packed firmly in the sample holder, leveled off at the upper edge to provide a smooth surface and transferred to the FTIR sample chamber (brief exposure to air).

Typical scan conditions were 1000 scans at ± 4 wavenumber resolution. All data are reported in Kubelka–Munk units, so that intensity values are nearly linear with concentration.

Electron microscopy. Both scanning (SEM) and transmission (TEM) electron microscopies were used to observe the powders. A Hitachi S800 with a field emission source was used at 10–15 keV with Au/Pd coated powders on an aluminum stub for SEM. A JEOL 2000FX was used at 200 keV with powders on a holey carbon grid for TEM. The TEM specimen was prepared by fluffing dry powder on to the grid. Note: fluffing dry powder is preferred over putting a droplet of suspension (in ethanol or hexane) onto the grid; because it was found that material tended to be deposited at capillaries created by particle contacts when the solvent dried.

Gas sorption. Surface areas and pore size distributions were determined by nitrogen adsorption at 77 K using the volumetric technique on a Micromeritics ASAP 2000M sorption analyzer (Norcross, GA). Samples were degassed at 110°C for 2 h, and then at 400°C until the outgas rate was less than 5 μm Hg min^{-1} (typically 4 h). The specific surface areas, SSA, were determined by the BET multipoint method with at least five data points with relative pressures between 0·001 and 0·20. Pore size distributions were determined using the density functional theory (DFT) using the nitrogen on carbon at 77 K, with slit-like pores model. Analysis was done with the software package supplied with the instrument.

Chemical analysis. Powders were submitted to The University of Michigan, Department of Chemistry analytical services, for analysis of carbon, hydrogen, and nitrogen content (CHN). A Perkin Elmer (Norwalk, CT) 2400 CHN Elemental Analyzer was operated at 1075°C, with He as a carrier gas. Powder specimens (1·5 mg) were loaded into tin capsules with powdered tin (6–10 mg) as a combustion aid. Acetanilide was used as a reference standard, and was analyzed in the same manner as the samples, with exception of omitting tin. Each powder was analyzed twice.

X-ray diffraction. Powder diffraction patterns were taken on a Rigaku (Tokyo, Japan) 2θ double crystal wide angle goniometer equipped with a rotating anode instrument with a Cu (K_α) source operated at 40 keV and 100 mA. Survey scans were taken at 10° 2θ min^{-1}, and peak scans were collected continuously at 1° 2θ min^{-1} at 0·05° 2θ intervals, and corrected to Si (111) (Cerac, Milwaukee, WI, -325 mesh). Grain size analysis was done according to the Scherrer equation, FWHM.[28] The JCPDS patterns used for comparison include anatase (21-1272) and rutile (21-1276).

Results

We present here the results of our titania UFP studies, beginning with the precursor development, followed by its conversion to an oxide powder by

flame spray pyrolysis. Finally, characterization of the UFP titania is presented and briefly compared to two related commercial powders: Degussa P25 and Nanophase titania.

Precursor development

Titanatrane glycolate synthesized via reaction (1) from the hydrosol and TEA may provide a useful Ti feedstock, due to the simplicity of the reaction scheme and the availability of the reagents. The synthesis and characterization of silatrane glycolate[29] provided the basis for developing the titanatrane analog. The product was characterized primarily by mass spectrometry;[29,30] however, analogous compounds have been synthesized previously.[3,13] The complex is miscible with many solvents (e.g. methyl, ethyl, and butyl alcohols). Most importantly, although no precautions were taken to avoid ambient air (moisture); the alkoxide showed no signs of hydrolysis after several months of storage. Titanatrane glycolate has a theoretical ceramic yield of 33·1 wt%; however, the $\approx$33 mol% excess TEA used in the synthesis leads to the lower ceramic yield (25 wt%) shown in the TGA (Fig. 2).

Titania preparation

The bulk precursor can be pyrolytically decomposed in air and ground to a fine powder to obtain titania powders; however, we are interested in producing ultrafine powders, which cannot be obtained by grinding. Thus, flame spray pyrolysis of titanatrane was used to produce the desired titania UFP. XRD analysis of the titania produced by FSP (Fig. 3) shows an anatase/rutile mixture containing roughly 10% rutile phase as determined from the relative intensities of the (1 0 1) anatase and (1 1 0) rutile peaks. BET analysis shows SSAs of $45 \pm 5\,m^2\,g^{-1}$. Equivalent spherical diameter (d_{esd}) calculations using SSAs and a

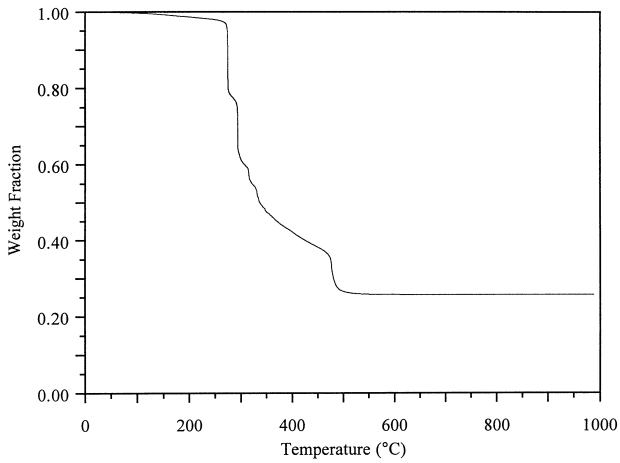

Fig. 2. TGA of titanatrane glycolate, 50°C min^{-1} HiRes 4 in air.

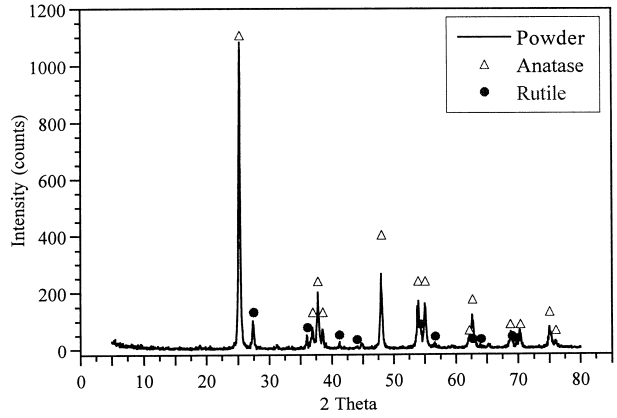

Fig. 3. Powder X-ray diffraction of flame spray pyrolyzed titania powder. JCPDS files shown are anatase (21-1272) and rutile (21-1276).

3·9 g cc^{-1} density determined by the rule of mixtures[29,31] give 34 ± 4 nm. Powder collected from the combustion chamber shows a higher rutile content (65%) and a lower SSA ($34\,m^2\,g^{-1}$), consistent with being held at higher temperatures. The Degussa P25 and Nanophase titania powders also consist of a mixture of $\approx$85% anatase and $\approx$15% rutile.

Particle sizes and morphologies were examined by electron microscopy (Fig. 4). The powders are uniform when viewed by SEM (a), where the image is free of large, porous particles characteristic of spray pyrolysis.[18] TEM (b) shows dense, spherical particles with some evidence of faceting. The particle sizes range from 10 to 100 nm, with the typical particle size $\approx$30 nm, showing good agreement with d_{esd}. Powder from the combustion chamber (c) shows enhanced faceting and necking. TEM of P25 (d) shows uniform particles that exhibit a high degree of necking and faceting. Both SEM (e) and TEM (f) micrographs of Nanophase UFP titania, showing spherical particles with a wide distribution in particle sizes (2–200 nm).

Powders produced by combustion may have products of combustion associated with them, either adsorbed or integrated into the material. The XRD shows that no accompanying phases develop as a result of the combustion process, so the only other concern is adsorbed species. The TGA profile and first derivative plot of as-produced FSP titania, Fig. 5, shows three main losses. These mass losses, when correlated with the FTIR analysis below, can be attributed to H_2O desorption. The first and largest mass loss (0·8 wt%, up to 120°C) arises from physisorbed H_2O. The second and third losses are attributed to loss of chemisorbed H_2O. The total losses up to 275° and 400°C are 1·3 and 1·4 wt%, respectively.

Figure 6 compares the DRIFTS of FSP titania with Degussa P25 and Nanophase titania.

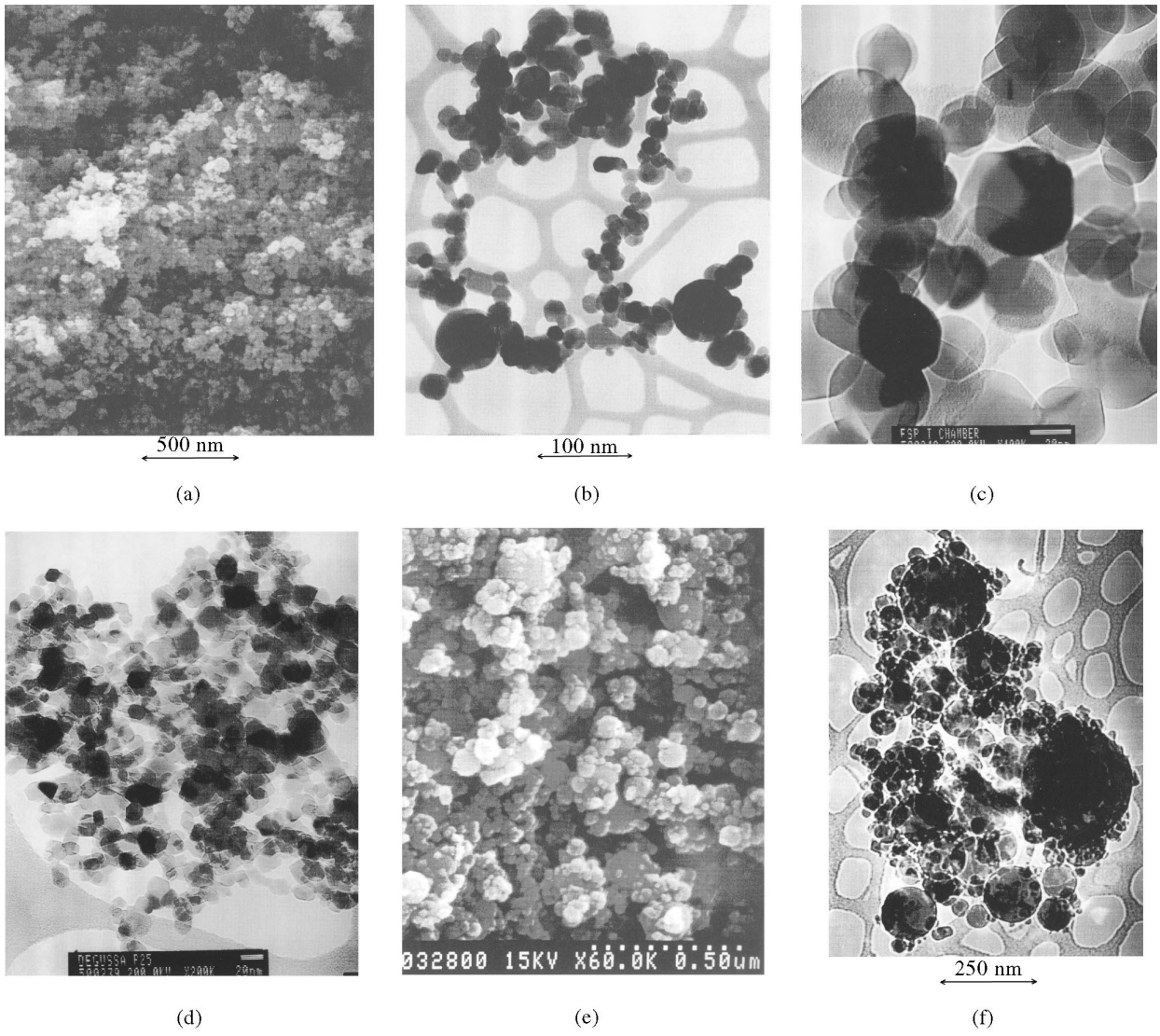

Fig. 4. Electron micrographs of ultrafine titania: (a) SEM of FSP powder; (b) TEM of FSP powder; (c) TEM of chamber FSP powder; (d) TEM of Degussa P25 powder; (e) SEM of Nanophase powder; and (f) TEM of Nanophase powder.

Absorptions due to (Ti–O) lattice vibrations show three main peaks at 710, 590, and 515 cm^{-1}. Maroni *et al.* ascribed the peak at 515 cm^{-1} to rutile (Eu).[32] The variation in relative intensities arises from the difference in the anatase/rutile ratio, as noted by XRD variations.

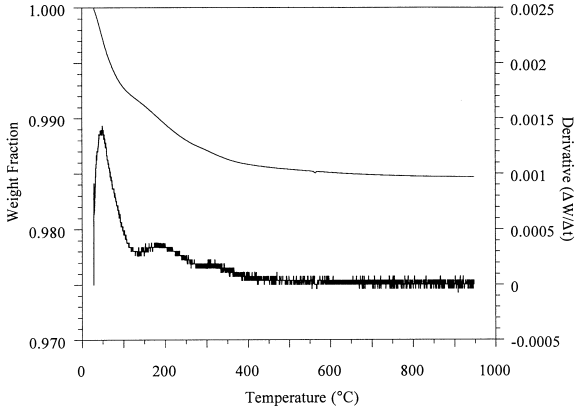

Fig. 5. TGA of FSP titania (air 10°C^{-1} min^{-1}) shown with derivative with respect to time.

The titania spectra are typical of high surface area powders, showing evidence of surface adsorbed species.[24,33–35] As suggested by the TGA, DRIFTS of the UFP titania surfaces reveal adsorbed H_2O. The fundamental IR absorptions of free H_2O occur at (ν_1) 3651, (ν_2) 1595, and (ν_3) 3756 cm^{-1}.[35] Adsorption shifts these bands as the molecular environment changes. Each spectrum shows evidence of H_2O in varying degrees. The broad peak at 3420 cm^{-1}, and the smaller peak at 1620 cm^{-1} are consistent with physisorbed, H-bonded molecular H_2O. These peaks diminish after vacuum heating at relatively low temperatures. Note that the intensities of these features are weak. Chemical analysis shows H contents less than the detection limit ($< 0{\cdot}2$ wt%) and the TGA loss up to 950°C is 1·6 wt% (0·17 wt% H, assuming all H_2O).

The sharp peak at 1380 cm^{-1} appears to be related to a surface species. Spectra of anatase and rutile with contaminated with surface oxo-anions show absorption in this vicinity, with shifts occurring

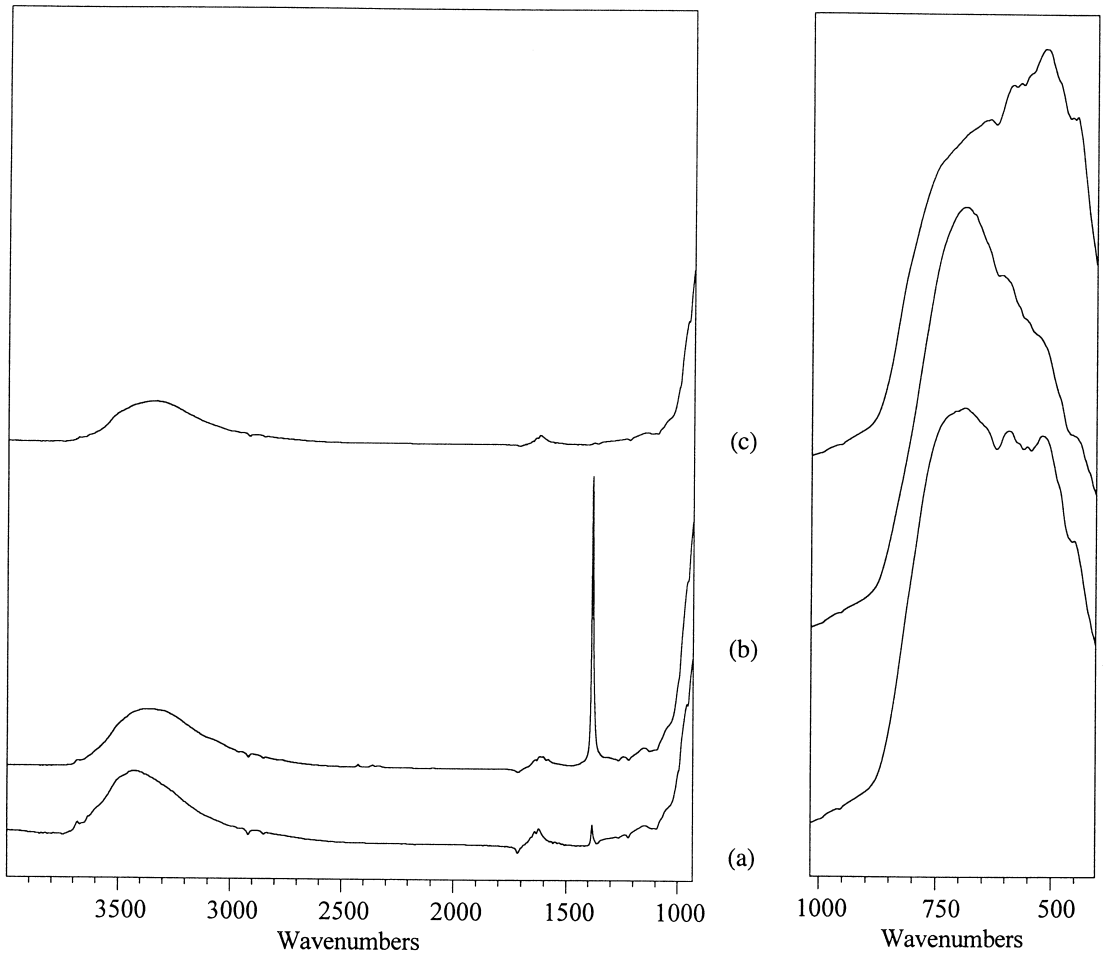

Fig. 6. DRIFTS of UFP titania. Shown are (a) FSP, (b) nanophase, and (c) P25 (intensity in KM units, 4000–1000 cm^{-1} region is 10× intensity of 1000–400 cm^{-1} region.)

according to the Ti oxidation state.[33–38] For example, TiO_2 surfaces doped with nitrate or sulfate exhibit peaks at 1370–80 cm^{-1}; additionally, ionized carboxyls are consistent with the 1380 and 1640 cm^{-1} peaks.[36–39] However, Morterra *et al.*[40] studied gas sorption on anatase, and proposed that CO_2 linearly chemisorbs on to Lewis acid sites, thereby weakly activating the IR- forbidden (Σ_g^+) mode at 1380 cm^{-1} of CO_2. Again, the intensity of this impurity peak is very low. Furthermore, chemical analysis shows the presence of C and N at or near the analysis detection limit (0·1–0·2 wt%), and the only known source of S is from mercaptan in the natural gas pilot torch. Thus, the exact source of this peak remains unknown; however, our results are consistent with a chemisorbed species such as CO_2 because after vacuum treatment the 1380 cm^{-1} peak diminishes.

The spectrum for Nanophase titania (4000–1000 cm^{-1}) is similar to that of the FSP powder, with the exception that the intensity of the 1380 cm^{-1} peak is greater, and there is a weak peak at 2425 cm^{-1}. Again, chemical analysis shows C, H and N are below the detection limits. Given that the Nanophase powder is produced under conditions essentially free from H_2O and CO_2, the observed spectrum must be the result of post-processing contamination. The spectrum of the Degussa P25 powder shows contributions from physisorbed H_2O noted by the broad ν(OH) centered at 3330 cm^{-1} and bending at 1620 cm^{-1} that both diminish after evacuation; however, the peaks ascribed to surface contamination are not seen.

Discussion

The objective of this research was to produce ultrafine titania powder via a processable titanium bearing precursor. Our approach was to:

1. first synthesize a processable precursor by a direct, simple technique;
2. then learn to control the solution behavior (viscosity) of the precursor for aerosolization;
3. use the precursor solutions for FSP of titania UFPs; and
4. finally characterize the resulting powders for further studies.

Discussion of these tasks follows accordingly.

Synthesis

Titanatrane synthesis by direct reaction of an oxide or hydroxide requires reaction of the components (TiO_2 and TEA) leading to digestion of the solid into the solvent. The reactivity was not the limiting issue, because reactions with pigment grade titania were successful; albeit in low reaction yields ($\approx$30 wt% in 6 h). Unfortunately, the unreacted components form an insoluble, highly viscous mass. Therefore, the focus of the synthesis procedure was to obtain a digestible raw material.

The reactivity of the starting material should scale with its cohesive energy; therefore, amorphous materials should react faster than crystalline materials. In both silatrane and alumatrane precursor syntheses,[3,29] faster reaction rates are obtained using amorphous rather than crystalline raw materials. Treadwell notes that solids precipitated from aqueous metal-salt solutions by ammonia are often amorphous, and are redissolved with either acids or bases; however, if brought to dryness, the solids crystallize.[41] Thus, precipitation of the aqueous metal-salt with ammonium carbonate should create a processing window for synthesis of the hydrosol without crystallization, allowing removal of the anion ($Cl-$) via washing. The resulting Ti hydrosol was X-ray amorphous.

The amorphous titania hydrosol produced by ammonium carbonate precipitation is a useful raw material for reaction (1) because formation of a soluble titanium alkoxide is favored over the formation of insoluble polymeric networks during synthesis. Titanatrane precursors synthesized by reacting triethanolamine with a titania hydrosol provide the opportunity to obtain high purity. Reaction (1) gives quantitative yields of titanatrane glycolate.[42] Consequently, the product purity is simply a function of the reagents used. The purity in this model case is determined by the $TiCl_4$ purity and our ability to minimize residual chloride in the hydrosol.

This synthetic route may prove quite versatile because hydrosols can be produced from many metal salts. For example, a hydrosol may be prepared by modification of the sulfate method for manufacturing pigment titania.[43] The sulfate process produces titanyl sulfate by digesting ilmenite ($FeTiO_3$) with sulfuric acid. The refined titanyl sulfate product may provide direct access to a titania hydrosol. The analogous alumatrane precursor can be prepared by reacting hydrosols derived from aluminum nitrate, aluminum sulfate or aluminum chloride with TEA.[42] The sulfate process has the advantage that lower grade ores can be used than required with the chloride route ($>85\%$ TiO_2). Although $TiCl_4$ was used in this model study, the choice of anion does not appear to be critical in the hydrosol formation, with the exception of ease of washing. Chloride is likely one of the more problematic choices, as triethanolamine hydrochloride forms with insufficient washing. Overall, the process provides a simple, direct route to a relatively stable titanium alkoxide precursor which is required for production of processable titania UFP.

Titania production

A pyrolysis process was sought that was free of process borne impurities. The combustion of an aerosol provides such an opportunity, because the aerosol provides a reactive, high surface area-to-volume fuel to an essentially a wall-less combustion process. The alcohol precursor solution provides organic matter to initiate and propagate the oxidative thermal conversion of the alkoxide to metal oxide clusters. This process differs significantly from spray pyrolysis,[18] and is more closely related to flame hydrolysis or flame combustion.[3,15–18,44]

There are three important aspects to flame spray pyrolysis: aerosol production, combustion, and powder collection. Although each aspect is modifiable, specific parameter changes may have ramifications on other aspects. For example, incomplete combustion occurs when large droplets are injected into the combustion zone, resulting in porous particles akin to those produced via spray pyrolysis.[18]

As stated above, the purpose of the aerosol is to inject the precursor into the combustion chamber as a high-surface-area-to-volume reactive droplet. Pyrolysis of the droplet may occur with or without mass transport (vaporization) of the solvent or the precursor. First, consider the case of solution pyrolysis without mass transport, where the droplet reacts to form a discrete, solid, spherical particle. The droplet size required to generate such a particle is given by eqn (2):

$$r_D = r_P \left(\frac{\rho_P}{Y \rho_D} \right)^{1/3} \tag{2}$$

where r is the radius, Y is the ceramic yield (wt%), ρ is the density, and the subscripts designate droplet and particle. Using eqn (2), the typical 35 nm ceramic particle generated by FSP would require an aerosol droplet diameter of 150 nm, much smaller than the 1–70 μm droplets generated by twin fluid aerosol generators.[4,5] In related work, Ocana showed that titania powders produced by aerosol hydrolysis of titanium alkoxides are an order of magnitude larger in diameter than the titania UFPs produced in this study.[45] Thus, mass transport must occur.

Mass transport can occur either via the vapor or liquid phase. In fuel oil combustion, vapor phase mass transport of fuel from the droplet surface results in a diffusion flame.[4,5,15] Flame spray pyrolysis does not vary much on changing from alcohol to precursor solution, except for an increase in luminescence. We believe that the precursor combustion mechanism is the same, especially considering that 75 vol% of the solution is alcohol. Titanatrane itself is not particularly volatile, as indicated by the TGA. Thus, direct vaporization of the precursor is not expected. However, the volatility of alcohol solvated titanatrane is unknown; and rapid heating (radiative, conductive, and convective) may vaporize the entire droplet upon injection into the combustion zone. The vaporized metal-alkoxide may then combust via a diffusion flame. Upon ligand combustion, the metal-alkoxide would yield a metal-oxide cluster free to nucleate and form the ensuing particles by condensation.

An alternate mechanism for mass transport is via the liquid phase, where the aerosol droplet is further divided by bursting, as a consequence of its rapid heating. Bursting may allow solution pyrolysis to form the final particles in accord with eqn (2).

The greatest constraints in the combustion process are associated with the various throughputs of the apparatus. The first limitation is the amount of heat that can be dissipated. Heat of combustion calculations from data in Table 1 show that the system produces >7 kW. Much of this energy is transferred via radiation, although some of the energy is carried along with the flue gases. There are two limitations concerning the flue gases: the quantity and its heat content. The by-product gases generated (CO_2 and H_2O) amount to 100–150 mol h^{-1} under typical conditions. This quantity equates to linear velocities of 0·5 m s^{-1} in the combustion zone and 0·1 m s^{-1} in the particle collectors and exhaust ducting, based on typical temperatures and geometry. The amount of heat carried by the flue gas to the powder collection system is partially controlled by the rate of gas removal. Maximum heat dissipation (read by lower thermocouple readings) occurs when the removal rate (controlled by a damper in the flue) is slightly greater than the gas generation rate.

Electrostatic precipitators (ESPs) and a countercurrent scrubber are used to collect powder. Under typical conditions, 75% of the powder is collected with ESPs. Powder collected in the scrubber is much more dispersed. Aqueous titania suspensions from the scrubber were stable (qualitatively) for more than three months. Powder collected in the ESPs are kept at >400°C in a humid environment; thus, it is likely that the particles are bonded beyond electrostatic attraction. The degree of interparticle bonding is not discernible from TEMs of ESP powder; however, an extreme is seen in TEMs of powders from the combustion chamber, where the particles are highly necked, and the phase assemblage is shifted to a higher rutile content.

Two commercial UFP titanias produced by vapor condensation techniques serve as benchmarks: Degussa P25 produced by flame hydrolysis of $TiCl_4$;[46] and Nanophase titania produced by vapor condensation of Ti vapor and subsequent oxidation to TiO_2.[6] Selected properties are shown in Table 2. Comparison of FSP titania with these powders shows similarities in the SSA. The major differences seen in the TEM micrographs appear to be: the particle size distribution, morphology, and interparticle contacts. Microscopy shows that stating a typical particle size, while appropriate for P25, does not describe the broad distributions seen in TEM of both FSP and Nanophase UFP titania. The P25 particles have a blocky morphology and are necked, indicating that the powder remained in a hot environment long enough for sintering to commence. Greater rutile content strengthens this claim, as rutile is the stable form at all temperatures.[43] Necking shields portions of the interparticle contacts, thus reducing the SSA. The Nanophase powder has a spherical morphology and shows particle sizes of 2–200 nm. The FSP powder from the ESPs has a more spherical morphology, with limited material at the neck region, while FSP chamber powder is similar to P25, having a blocky morphology.

Summary

A chelated metal–alkoxide precursor, titanatrane glycolate, was synthesized by reacting a titania hydrosol with triethanolamine in ethylene glycol. Titanium tetrachloride was used as the titanium

Table 2. Selected properties comparing flame spray pyrolyzed titania with flame hydrolyzed titania

	XRD phase assemblage (anatase/rutile)	*Specific surface area ($m^2 g^{-1}$)*	*Particle size*		*Particle morphology*
			d^{esd}	$d^{typical}$	
FSP ESP	90/10	45	35	30	Spherical
Chamber	35/65	34	50		Blocky
P25	85/15	50	31	20	Blocky
Nanophase	85/15	47	33		Spherical

source for the hydrosol; however, other metal salts are candidates for further investigation. Titanatrane is soluble in alcohols and shows stability against hydrolysis. This precursor was used as the feedstock for producing ultrafine titania particles by flame spray pyrolysis, at rates greater than $25\,g\,h^{-1}$. The oxide product was an approximately 90/10 anatase/rutile, $45\,m^2\,g^{-1}$ powder with typical particle size of 35 nm. This technique may be a useful alternative to flame hydrolysis of the metal chloride. These powders provide an excellent starting point for processing TiN as well.

Acknowledgements

We would like to thank the Army Materials Laboratory through contract No. DAAL01-93-M-S522 and NASA through co-operative research agreement NLRC NCC3-381 for support of this work.

References

1. Gallas, M. R., Hockey, B., Pechenik, A. and Piermarini, G. J., Fabrication of transparent γ-Al_2O_3 from nanosize particles. *J. Am. Ceram. Soc.*, 1994, **77**, 2107–2112.
2. Kuhn, W. E., Lamprey, H. and Sheer, C., *Ultrafine Particles*. Wiley, New York, 1963.
3. Bickmore, C. R., Waldner, K. F., Treadwell, D. R. and Laine, R. M., Ultrafine spinel powders by flame spray pyrolysis of a magnesium aluminum double alkoxide. *J. Am. Ceram. Soc.*, 1996, **79**, 1419–1423.
4. Williams, A., *Combustion of Liquid Fuel Sprays*. Butterworths, Boston, 1990, p. 206.
5. Lefebvre, A. H., *Atomization and Sprays*, Hemisphere, New York, 1989, p. 19.
6. Siegel, R. W., Ramasamy, S., Hahn, H., Zongquan, L., Ting, L. and Gronsky, R., Synthesis, characterization, and properties of nanophase TiO_2. *J. Mater. Res.*, 1988, **3**, 1367–1372.
7. Everest, D. A., Sayce, I. G. and Selton, B., Preparation of ultrafine alumina powders by plasma evaporation. *J. Mater. Sci.*, 1971, **6**, 218–224.
8. Nielsen, M. L., Hamilton, P. M. and Walsh, R. J., Ultrafine metal oxides by decomposition of salts in a flame. In *Ultrafine Particles*, ed. W. E. Kuhn, H. Lamprey and C. Sheen. Wiley, New York, 1963, pp. 181–195.
9. Kamal, A. M., Vemury, S. and Pratsinis, S. E., Competition between $TiCl_4$ hydrolysis and oxidation and its effect on product TiO_2 powder. *AIChE J.*, 1994, **40**, 1183–1192.
10. Sokolowski, M., Sokolowska, A., Michalski, A. and Gokieli, B., The 'in-flame-reaction' method for Al_2O_3 aerosol formation. *J. Aerosol Sci.*, 1977, **8**, 219–230.
11. Lewis, D. J., Technique for producing mullite and other mixed-oxide systems. *J. Am. Ceram. Soc.*, 1991, **74**, 2410–2413.
12. Bradley, D. C., Mehrotra, R. C. and Gaur, D. P., *Metal Alkoxides*. Academic Press, New York, 1978, pp. 226–241.
13. Tyzor®, Organic Titanates. Technical Information, DuPont Specialty Chem., Deep Water, NJ.
14. Glassman, I., *Combustion*. Academic Press, New York, 1977.
15. Ulrich, G. D., Flame synthesis of fine particles. *Chem. and Eng. News*, 1984, 22–29.
16. Flagan, R. C., Aerosol Routes for Powder Synthesis. In *Ceramic Transactions. Ceramic Powder Science II*, ed. G. L. Messing, E. R. Fuller and H. Hausner. Am. Ceram. Soc., Westerville, OH, 1987, pp. 229–243.
17. Kodas, T. T. and Sood, A., Alumina powder production by aerosol processes. In *Alumina Chemical, Science and Technology Handbook*, ed. L. D. Hart. Am. Ceram. Soc. Westerville, OH, 1990, pp. 375–383.
18. Messing, G. L., Zhang, S-C. and Jayanthi, G. V., Ceramic powder synthesis by spray pyrolysis. *J. Am. Ceram. Soc.*, 1993, **76**, 2707–2726.
19. Pena, M. V-R. J., Martinez, A. and Gonzalez-Calbet, J. M., Selection of structural type and particle size in titanium (IV) oxide. *J. Mater. Res.*, 1993, **8**, 2336–2343.
20. Fletcher, M., ARL, pers. comm.
21. Laine, R. M., Treadwell, D. R., Mueller, B. L., Bickmore, C. R., Waldner, K. F. and Hinklin, T., Processable aluminosilicate alkoxide precursors from metal oxides and hydroxides. The oxide one pot synthesis (OOPS) process. *J. Chem. Mater.*, 1996, **6**, 1441–1443.
22. Laine, R. M., Mueller, B. L., Hinklin, T., Neutral and mixed neutral/anionic polymetalloxanes, US Patent No. 5 418 298, 1995.
23. *CRC Handbook of Chemistry and Physics*, 58th ed., ed. R. C. Weast, CRC Press, 1977, F245.
24. Jones, P. and Hockey, J. A., Infra-red studies of rutile surfaces, Part 1. *Trans. Faraday Soc.*, 1971, **67**, 2669–2678.
25. Urban, M. W., Koenig, J. L., Recent developments in depth profiling from surfaces using FT-IR spectroscopy. In *Vibrational Spectra and Structure: A Series of Advances Volume 18, Applications of FT-IR Spectroscopy*, ed. J. R. Durig. Elsevier, New York, 1990.
26. Gaskell, P. H. Models for the Structure of Amorphous Solids. In *Materials Science and Technology, A Comprehensive Treatment: Glasses and Amorphous Materials*, ed. R. W. Cahn, P. Haasen, E. J. Kramer and J. Zarzycki (vol. ed.). **9** VCH, New York, 1991.
27. Pavia, D. L., Lampman, G. M. and Kriz, G. S. Jr, *Introduction to Spectroscopy: A Guide for Students of Organic Chemistry*. Saunders College, Orlando, 1979.
28. Cullity, B. D., *Elements of X-Ray Diffraction*, 2nd ed. Addison-Wesley, Reading, MA, 1978.
29. (a) See Ref. 21, and (b) Bickmore, C. R. and Laine, R. M., Processing Oxynitride Powders via Fluidized Bed Ammonolysis of Large, Porous, Silica Particles. *J. Am. Ceram. Soc.*, 1996, **79**, 2865–2877.
30. Waldner, K. F., Masters thesis, University of Michigan, 1995.
31. Ninety per cent anatase (3.84 g/cc) and 10% rutile (4.26 g/cc) gives 3.9 g/cc.
32. Maroni, V. A., Valence force field treatment of the rutile structure at zero-wave vector. *J. Phys. Chem. Solids*, 1988, **49**, 307–313.
33. Yates, D. J. C., Infrared studies of the surface hydroxyl groups on titanium dioxide, and of the chemisorption of carbon monoxide and carbon dioxide. *J. Phys. Chem.*, 1961, **65**, 746–753.
34. Busca, G., Saussey, H., Saur, O., Lavalley, J. C. and Lorenzelli, V., FT-IR characterization of the surface acidity of different titanium dioxide anatase preparations. *Applied Catalysis*, 1985, **14**, 245–260.
35. Hair, M. L., *Infrared Spectroscopy in Surface Chemistry*. Marcel Dekker, New York, 1967.
36. Kantcheva, M. M., Bushev, V.Ph. and Hadjilvanov, K. I., Nitrogen dioxide adsorption on deuteroxylated titania (anatase). *Trans. Faraday Soc.*, 1992, **88**, 3087–3089.
37. Lewis, K. E. and Parfitt, G. D., Infrared study of the surface of rutile. *Trans. Faraday Soc.*, 1966, **62**, 204–214.
38. Knozinger, H., Specific poisoning and characterization of catalytically active oxide surfaces. *Advances in Catalysis*, ed. D. D. Edley, H. Pines and P. B. Weisz. Academic Press, New York, 1976, **25**, pp. 184–271.

39. Drago, R. S., *Physical Methods in Chemistry*. W. B. Saunders, Philadelphia, 1977, p. 167.
40. Morterra, C., Chiorino, A., Boccuzzi, F. and Fisicaro, E., A spectroscopic study of anatase properties, 4. The adsorption of carbon dioxide. *Z. Phys. Chem.*, 1981, **124S**, 211–222.
41. Treadwell, F. P. and Hall, W. J., *Analytical Chemistry Vol. I, Qualitative Analysis*, 9th edn. Wiley, New York, 1937, pp. 548–549.
42. Bickmore, C. R., Ph.D. dissertation, University of Michigan, 1996.
43. Whitehead, J., Titanium compounds. In *Kirk-Othmer Encyclopedia of Chemical Technology*, Vol. 23. John Wiley and Sons, Inc., New York, 1978, pp. 131–176.
44. Barnard, J. A. and Bradley, J. N., *Flame and Combustion*, 2nd edn. Chapman and Hall, New York, 1985, p. 256.
45. Ocana, M., Fornes, V. and Serna, C. J., A simple procedure for the preparation of spherical oxide particles by hydrolysis of aerosols. *Ceram. Int.*, 1992, **18**, 99–106.
46. Degussa Technical Bulletins, (a) **60** 2nd edn, 1986; and (b) **56**, 6th edn, 1993.